

# A Comparative Study on Tensile and Fracture Behavior of Al–Mg Alloy Processed Through Cryorolling and Cryo Groove Rolling

K. K. Yogesha<sup>1</sup> · Nikhil Kumar<sup>1</sup> · Amit Joshi<sup>1</sup> ·  
R. Jayaganthan<sup>1,2</sup> · S. K. Nath<sup>1</sup>

Received: 29 January 2016/Revised: 12 April 2016/Accepted: 15 April 2016/Published online: 10 May 2016  
© Springer Science+Business Media New York and ASM International 2016

**Abstract** In the present work, Al–Mg alloy (AA 5052) was subjected to cryorolling followed by post-deformation annealing, in order to investigate its effect on tensile and fracture behavior. The solution-treated Al alloys were cryorolled (CR) and cryo groove rolled to different true strains. The microstructure of the samples (deformed and post-annealed) was characterized by optical microscopy, x-ray diffraction, and TEM to substantiate the mechanisms of grain refinement and its influence on tensile and fracture properties. Fractography of the tensile as well as three-point bending test samples was carried out using a scanning electron microscope (SEM) to reveal the fracture mode. The deformed samples (90% thickness reduction) exhibit significant improvement in strength (291 MPa) and hardness (110 HV) in CR samples and 313 MPa and 122 HV in cryo groove rolled samples, which is due to high dislocation density and grain size reduction. Post-annealing of the deformed samples (90% thickness reduction) led to improvement in its ductility as well as fracture toughness. The cryo groove rolled samples and post-annealed samples have shown better fracture toughness (142 kJ/m<sup>2</sup>) as compared to cryo rolled samples (29 kJ/m<sup>2</sup>) due to the relatively

larger grain and dimples as observed from TEM and fractography studies.

**Keywords** Groove rolling · Fracture strength · Microstructure · Fractography

## Introduction

Aluminum alloys with ultrafine grained (grain size between 100 and 1000 nm) microstructure exhibit better strength, fatigue strength when compared to its bulk alloys [1]. AA 5052 has been studied extensively and they show good combination of mechanical properties such as tensile strength, fatigue strength, and fracture toughness. It is used in marine applications, automotive components, food processing equipment, as well as in aircraft components. The improvement in strength of this alloy is achieved through solid solution strengthening and work hardening. Severe plastic deformation (SPD) is one of the novel thermo-mechanical processing techniques used for producing ultrafine grain microstructure (UFG) with superior mechanical properties in ferrous and non-ferrous alloy [2]. SPD techniques such as Accumulative roll bonding (ARB) [3–9], Equal channel angular pressing (ECAP) [10–16], Multi-axial forging (MAF) [17–21], Repetitive corrugation and straightening (RCS) [22–27], High-pressure torsion (HPT) [28–34], are routinely used for producing ultrafine grain materials; however, the limitations associated with these techniques for large-scale products are due to requirement of severe plastic strain of the order of 5 or 6 at ambient or elevated temperatures, expensive tooling, and design difficulties. Hence, they are confined to mainly for producing small-length scale products. Alternative to the SPD techniques,

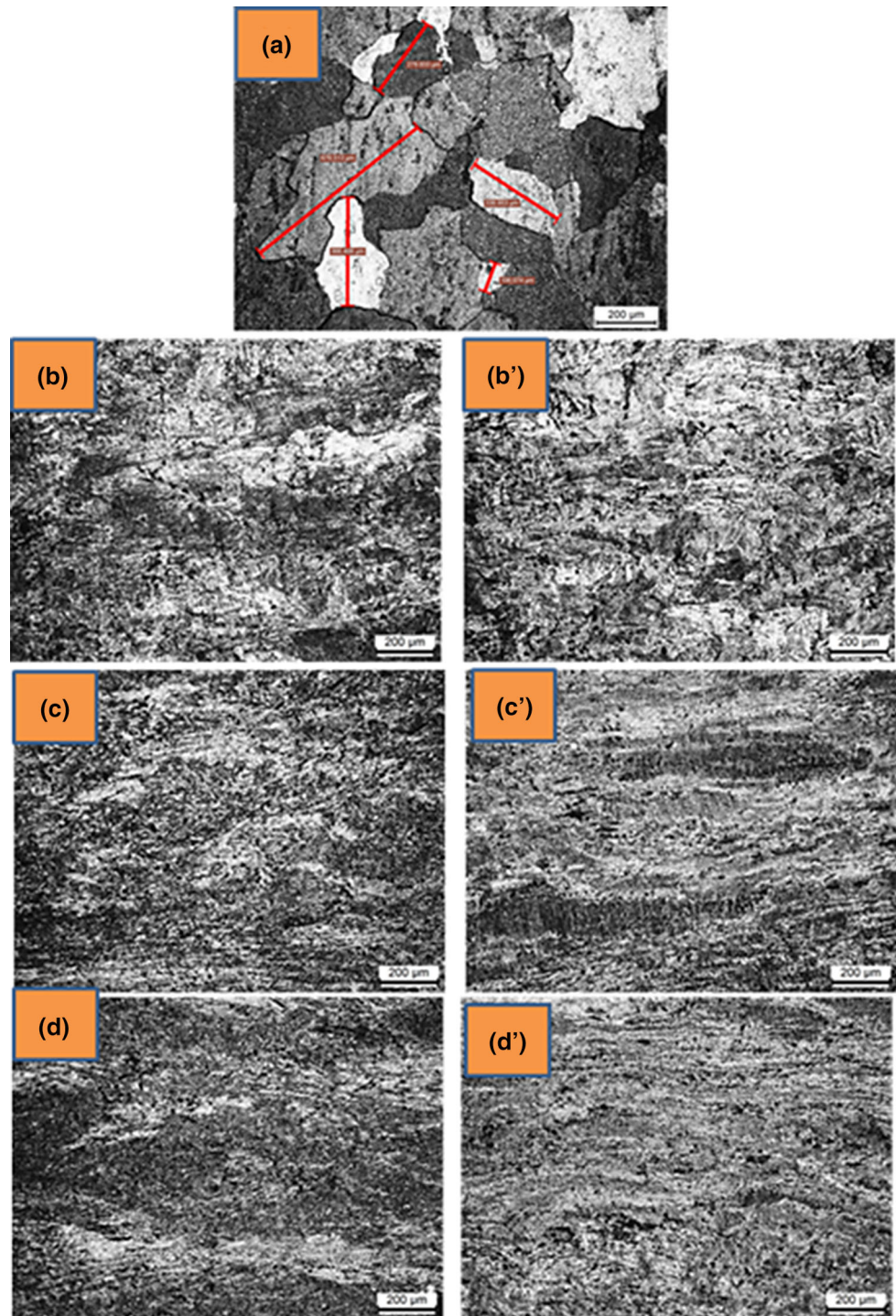
✉ R. Jayaganthan  
rjayafmt@iitr.ernet.in; metarj@iitm.ac.in

<sup>1</sup> Department of Metallurgical and Materials Engineering & Centre of Nanotechnology, Indian Institute of Technology Roorkee, Roorkee 247667, India

<sup>2</sup> Department of Engineering Design, Indian Institute of Technology Madras, Chennai 600036, India

**Table 1** Compositional details of AA 5052

Element	Si	Fe	Cu	Mn	Mg	Cr	Zn	Al
Composition, (wt%)	0.20	0.33	0.10	0.10	2.3	0.26	0.10	Remainder

**Fig. 1** Optical micrographs; (a) starting material (ST), (b) 50% CR, (c) 75% CR, (d) 90% CR (b') 50% CGR, (c') 75% CGR, (d') 90% CGR

**Fig. 2** Variation in (a) UTS (b) YS and (c) Elongation in CR and CGR samples with respect to rolling condition

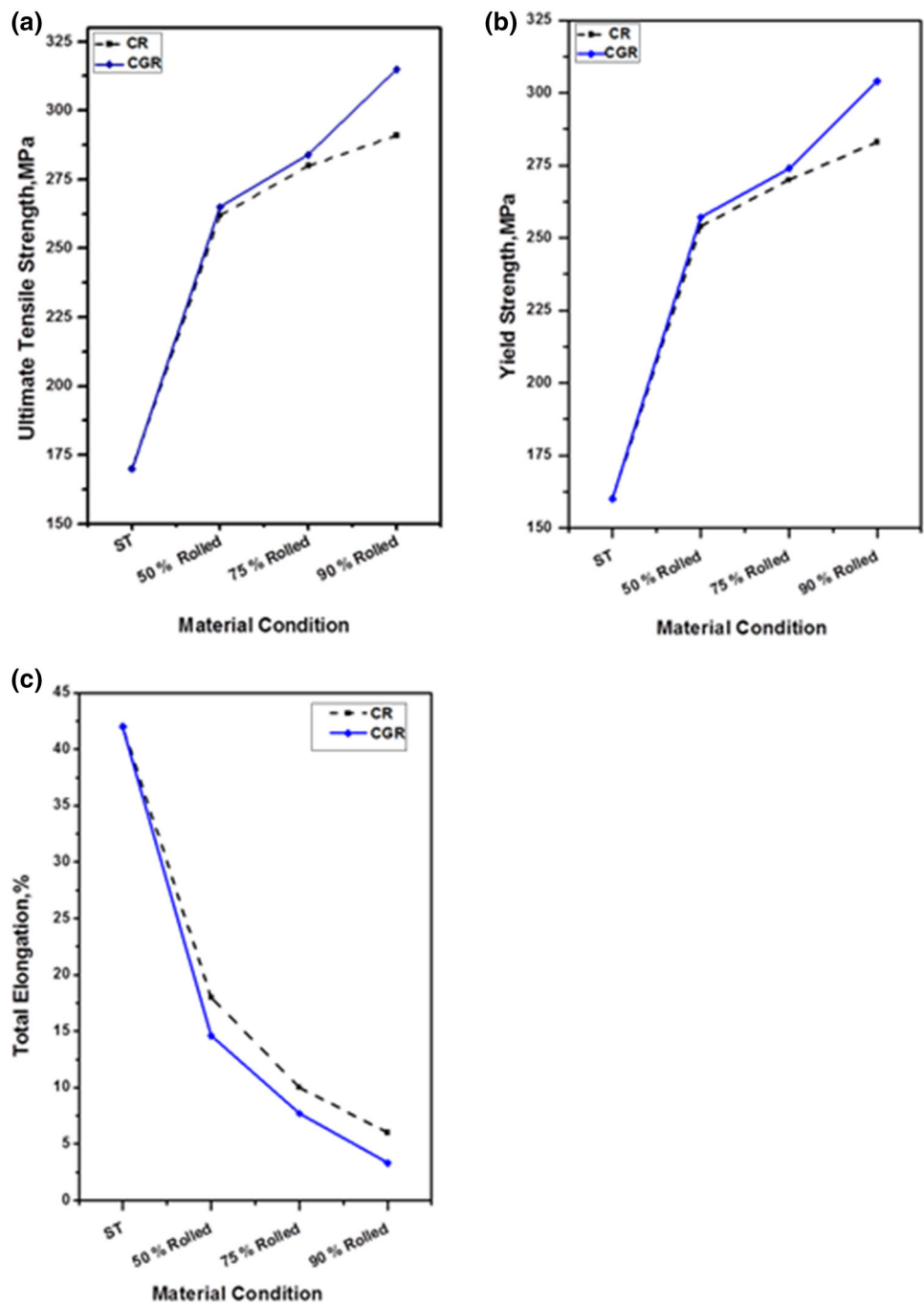


**Table 2** Mechanical properties of AA 5052 after CR, CGR process

Material condition	Hardness (HV)	UTS (MPa)	YS (MPa)	Total elongation (%)
ST	55	170	160	42
50% CR	94	262	254	18
50% CGR	105	265	255	14.6
75% CR	97	280	270	10
75% CGR	112	284	274	7.7
90% CR	110	291	283	6
90% CGR	122	315	304	3

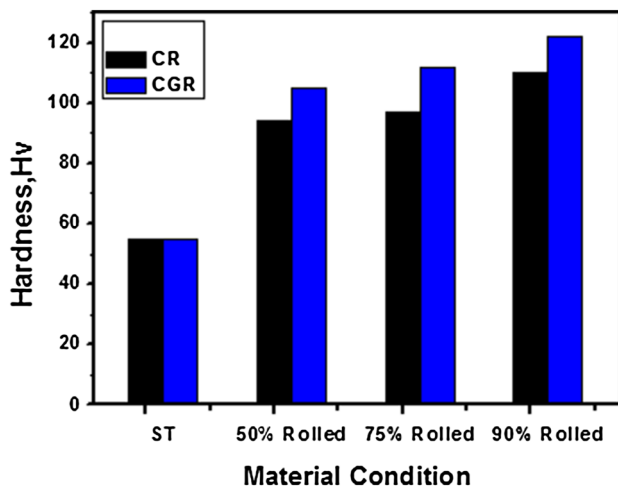


**Fig. 3** Variation in Hardness (Vicker's Hardness value) with respect to rolling condition

cryorolling has been identified as a potential route to produce UFG microstructures in the light metals and alloys [1, 2, 35–40]. The suppression of dynamic recovery at cryogenic temperature is responsible for enhanced grain refinement during cryorolling. It requires less plastic deformation when compared to other SPD techniques at ambient or elevated temperatures for producing ultrafine grains. Kang et al. have performed the cryorolling followed by warm rolling of AA 5052 between temperature range 448 and 573 K and reported that cryorolling followed by warm rolling at 448 K was much more effective in improving the tensile strength up to 452 MPa [2]. It was attributed to the formation of fine precipitates, about 50–100 nm in diameter. They also observed that the subsequent annealing of such samples at 448 K for 48 h resulted in high ductility, due to the formation of fine equiaxed grains of size 100–200 nm and reduction in dislocation density. Cryogenic rolling of AA 5052 with 85% reduction followed by annealing treatment between temperatures 150 to 300 °C has shown increment in its

elongation above 250 °C as reported in the literature [35]. It is closely related to the annihilation of mobile dislocations during annealing and the increased amount of coarse equiaxed grains. Recently, Wang et al. have investigated the AA 5052 subjected to cold rolling followed by annealing treatment between the temperature range of 220 to 380 °C [41]. It was reported in their work that the ultimate tensile strength has increased up to 325 MPa at 87% thickness reduction due to work hardening during cold rolling process. The post-annealed samples treated between the temperatures 220 to 380 °C have shown abundant precipitates of  $Mg_2Al_3$  in their work. Lee et al. have performed constrained groove rolling for refinement of grains in pure Al by shear deformation [42]. Krisnaiah et al. have conducted groove pressing of pure Al at room temperature as well as cryogenic temperature and reported the improvement in UTS from 79 to 96 MPa [43]. Fang et al. have investigated ECAP processed Al–Mg alloy and reported that the static toughness decreases significantly after one ECAP pass, which is due to decrease in elongation than its casting state, though its strength is obviously increased [13]. Zonghoon et al. have produced UFG Al–Mg alloy by cryomilling process and reported that coarse grained, bimodal alloys show better fracture toughness than UFG alloys as they resist crack growth by bridging of crack wakes, and obstructing crack propagation by deflecting and splitting of crack tips and by delamination during plastic deformation [44]. However, the literature on fracture properties of cryorolled and groove rolled AA 5052 is limited. Hence, the present work is envisaged to study the influence of cryorolling as well as cryo groove rolling and post-annealing treatment on tensile strength and fracture behavior of AA 5052. The detailed microstructural investigations of the deformed and annealed alloys were made through SEM and TEM to substantiate the improvement in mechanical properties observed in the present work.

**Fig. 4** SEM fractographs of AA 5052 after Tensile test (a) Bulk alloy (as received material) (b) ST

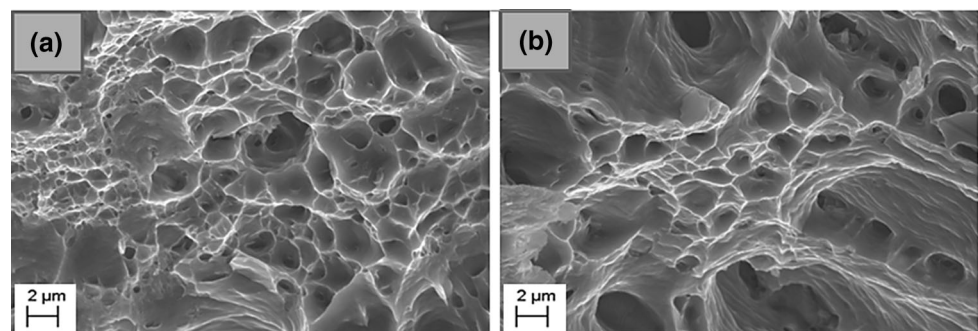
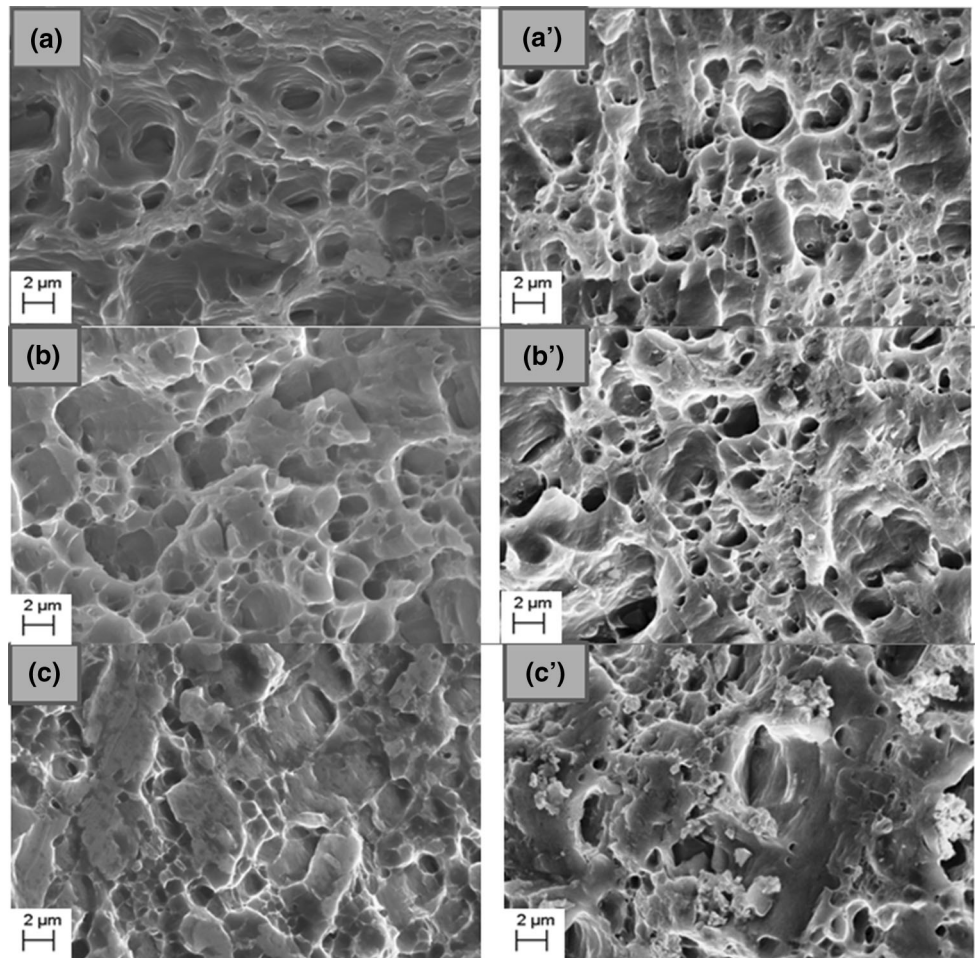


**Fig. 5** SEM fractographs of AA 5052 after Tensile test (a) 50%CR, (b) 75%CR (c) 90%CR, (a') 50%CGR, (b') 75%CGR (c') 90%CGR



### Experimental Procedure

#### Processing

The commercially available AA 5052 with chemical composition 2.3 wt% Mg, 0.26 wt% Cr, 0.2 wt% Si, 0.33 wt% Fe, 0.10 wt% Cu, 0.10 wt% Mn, 0.10 wt% Zn, and rest aluminum is shown in Table 1. The samples were prepared from the received material to the dimension  $30 \times 40 \times 10 \text{ mm}^3$  and annealed at  $540 \text{ }^\circ\text{C}$  for 2 h followed by water quenching. Subsequently, one set of samples is rolled into three different true strains of 0.69, 1.38, and 2.3 (50, 75, and 90% thickness reduction) at cryogenic temperature. Cryorolling of AA 5052 plate was carried out by dipping it in liquid nitrogen for 15 min prior to each roll pass. Similarly, other set of samples is groove rolled (70%) followed by flat rolling (30%) to same thickness reduction (50,75 and 90%) in cryogenic temperature. The homogeneity during the deformation was maintained by

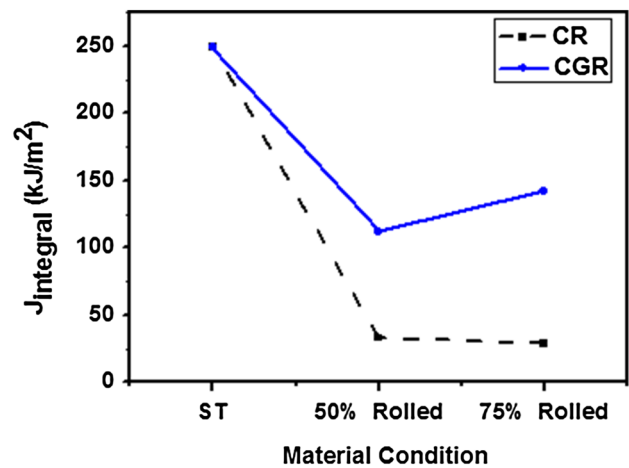
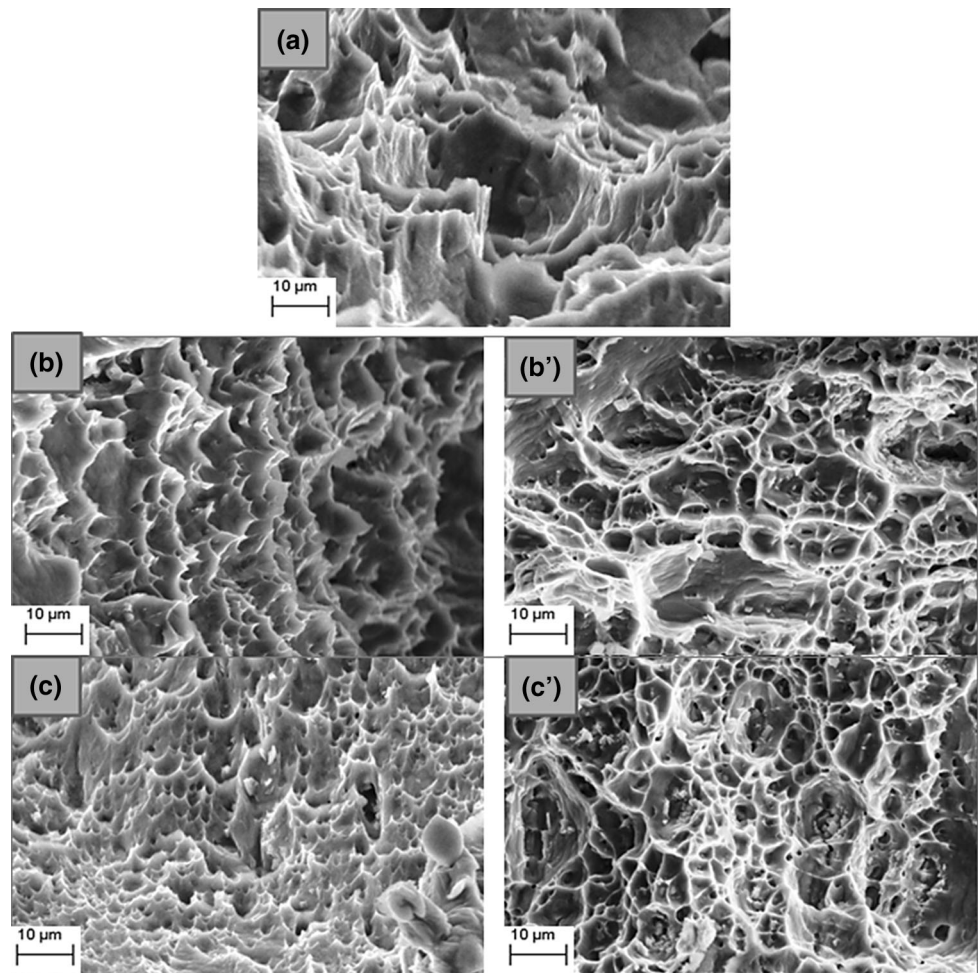


**Fig. 6** Variation in  $J_{\text{integral}}$  with respect to rolling condition

reversing the surface (upside down) of the sample after each pass to ensure reverse shear deformation of the deformed zone [42].

**Fig. 7** SEM fractographs of AA 5052 after three-point bending test (a) ST, (b) 50%CR, (c) 75%CR (b') 50% CGR (c') 75%CGR



### Tensile and Hardness Measurements

Tensile testing and microhardness testing of the samples were conducted at different thickness reductions to study the influence of deformation strain on the grain refinement. To optimize the tensile properties, annealing was performed at 180–300 °C for 1 h. Tensile test samples were prepared as per the ASTM Standard E-8/E8M-09 sub-size specimen of gage length 25 mm. The tensile test was conducted on a universal testing machine using a strain rate of  $0.6 \times 10^{-3}$ /s. The Vickers hardness testing was made on plane parallel to the direction of rolling with a load of 5 kgf for a dwell time of 15 s.

### Fracture Toughness

Single-edge notch bend (SENB) test samples for span length of 30 mm were prepared as per the ASTM E1820 standard to perform three-point bending test in order to evaluate fracture toughness. The microstructures of the solution-treated (ST), cryorolled, cryo groove rolled, and

post-annealed samples were characterized using an optical microscope. Modified Poulton's reagent was used for etching the polished samples to get optical micrographs of the processed samples. TEM samples were prepared by thinning down the samples up to 80 μm thickness and punching it into 3 mm diameter, followed by twin-jet polishing in the solution of 20% perchloric acid and 80% methanol maintained at  $-40$  °C using 40 V DC supply [1]. TEM characterization of the samples was performed using an operating voltage of 200 kV. XRD characterization of ST, processed, and post-annealed samples were performed on x-ray diffractometer with operating voltage of 40 kV and 30 mA current.

## Results and Discussion

### Microstructural Characteristics

The solution-treated samples possess equiaxed grains of size 352 μm as shown in Fig. 1. The second-phase

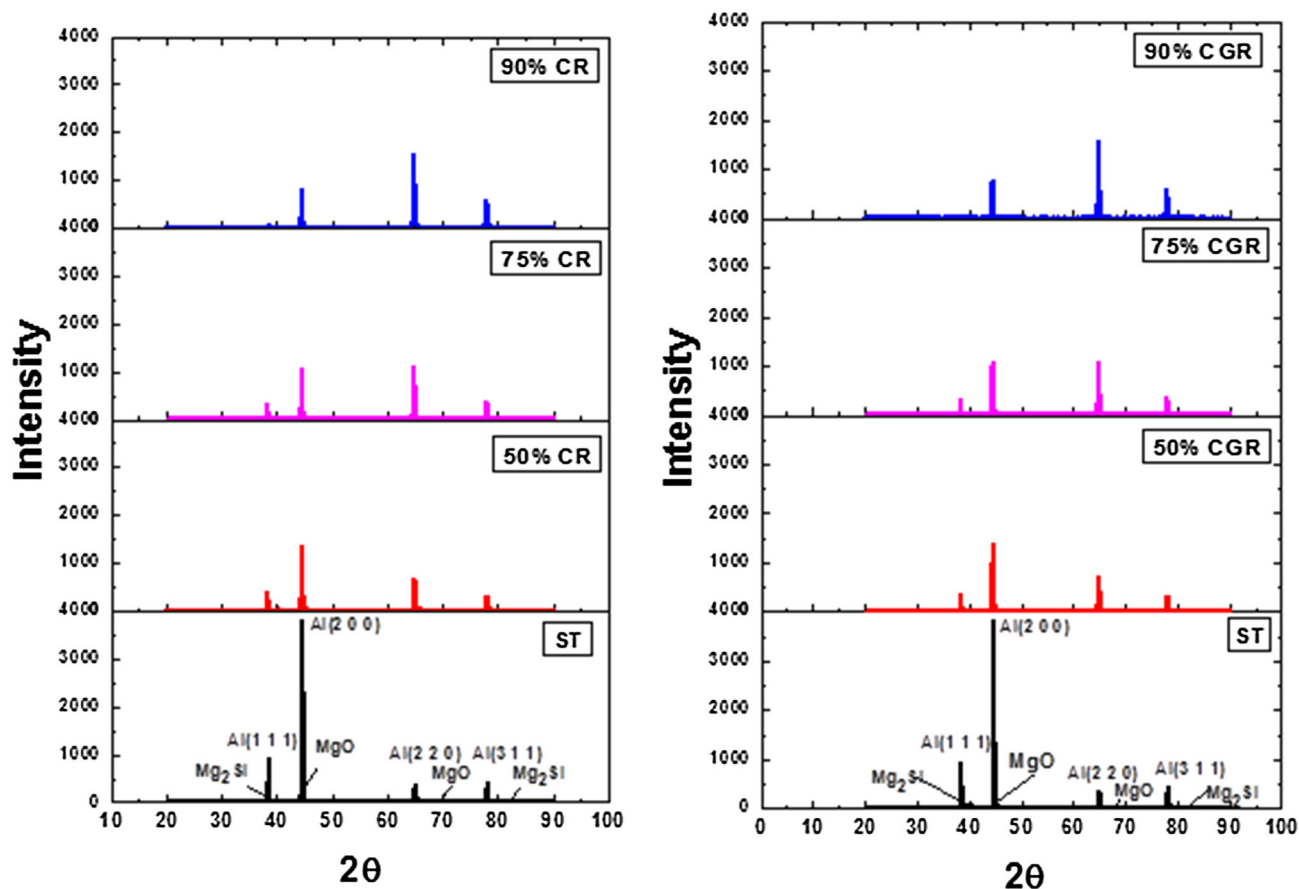


Fig. 8 XRD pattern of AA 5052 at different deformation conditions

impurity particles are also seen on the coarse grains. In 50 and 75% CR samples, the elongated grains with accumulation of dislocation are seen, whereas the 90% CR sample, shows more deformed elongated structure with high density of dislocations. In case of CGR samples, due to combined compressive and shear stress, the material is deformed much more severely than CR samples and therefore, it reveals higher density of dislocation. The fine impurity phase particles present in the material promotes dislocation accumulation by becoming obstacle for the dislocation movement.

### Tensile Properties

The tensile strength (UTS) and yield strength (YS) are increased from 170 to 291 MPa and 160 to 283 MPa, respectively, for the 90% CR sample as shown in Fig. 2 and Table 2. However, the percentage elongation to failure has decreased from 39 to 6%. In case of 90% CGR samples, the yield strength and tensile strength are 304 and

315 MPa, respectively, whereas the percentage elongation to failure has decreased to 3%, which is the distinctive behavior of cold-worked samples. The increase in tensile strength was attributed to high dislocation density accumulated during CR/CGR process.

The hardness has increased from 55 to 110 HV for 90% CR sample, whereas in case of 90% CGR sample, it is 122 HV (Fig. 3). It is due to effective strain hardening of the material during CGR process than CR process. The enhancement of the hardness is attributed to high dislocation density generated in the samples during rolling and effective suppression of cross slip or climb of dislocation associated with dynamic recovery [36].

The SEM fractography (Fig. 4) of the tensile test samples clearly shows that the ST samples with large dimple size and with cavities of different size, which indicate the ductile fracture, whereas in 50, 75, and 90% CR samples, the dimple size is getting finer (Fig. 5), revealing the mixed mode of fracture. In case of CGR samples, the dimples are still fine and possessing much more cleavage surface than CR samples.

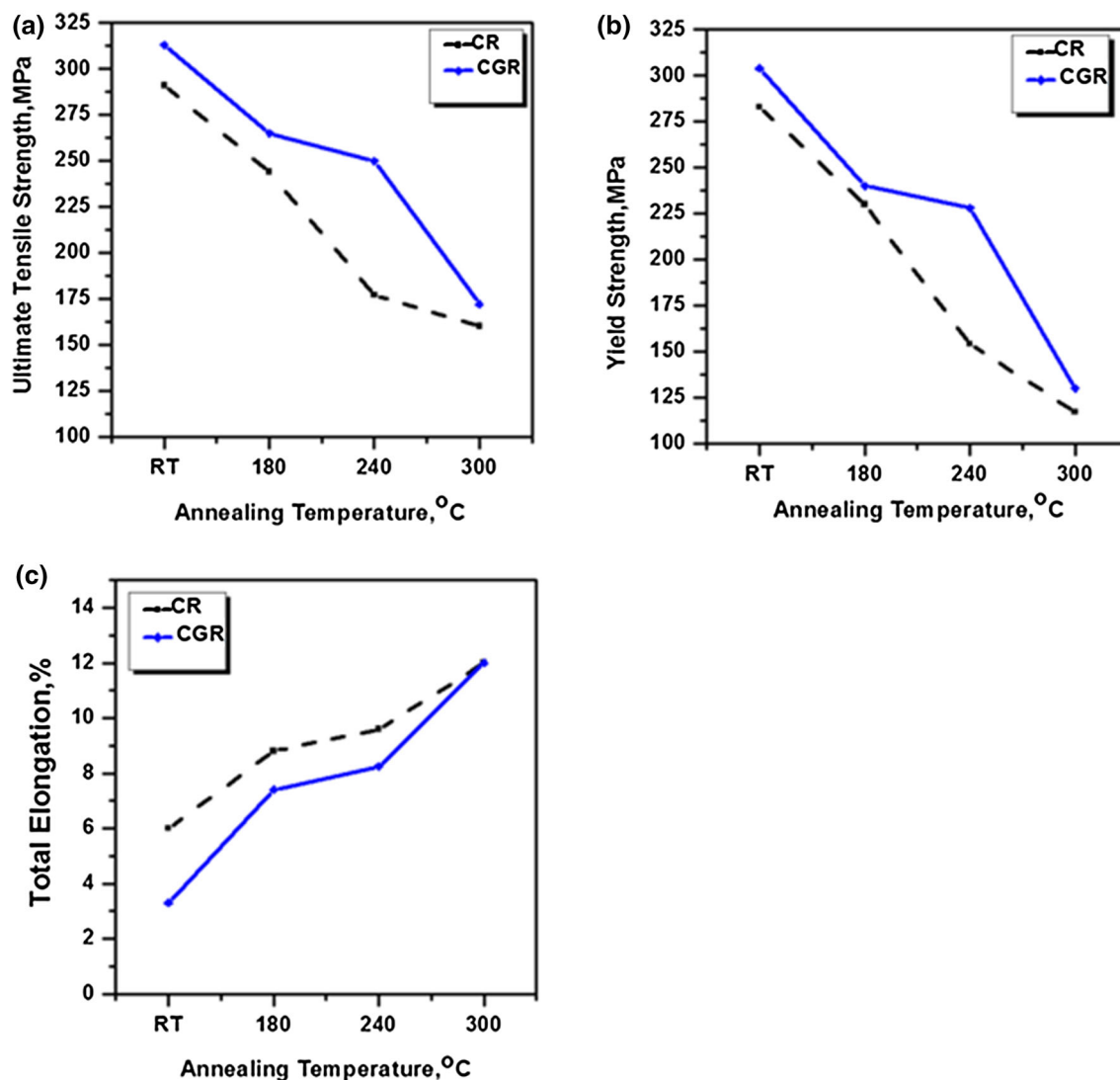


**Fig. 9** Effect of annealing temperature on tensile properties of 90% rolled and annealed for 1 h. Variation in (a) UTS (b) YS and (c) elongation in CR and CGR samples at different annealing temperature

**Table 3** Mechanical properties of 90% CR, CGR of AA 5052 after post-deformation annealing treatment at different temperatures

Material condition	Hardness (HV)	UTS (MPa)	YS (MPa)	Total elongation (%)
90% CR + 180 °C	101	244	230	8.8
90% CGR + 180 °C	112	265	240	7.4
90% CR + 240 °C	92	180	154	9.6
90% CGR + 240 °C	10	250	228	8.25
90% CR + 300 °C	82	160	117	12
90% CGR + 300 °C	88	172	130	12

### Fracture Toughness

The apparent fracture toughness,  $J$  is calculated from the following relation [45, 46],

$$J = \frac{2A}{Bb} = \frac{2}{Bb} \int_0^{u_{\max}} P \, du,$$

where  $A$  is the area under load–displacement curve,  $B$  is the specimen thickness,  $b$  is the unbroken ligament ( $W-a$ ), and  $u_{\max}$  denotes the displacement at which the load ( $P$ ) reaches maximum value.

The fracture toughness in terms of  $J_{\text{integral}}$  values for the 75% CR samples (Fig. 6) has decreased when compared to



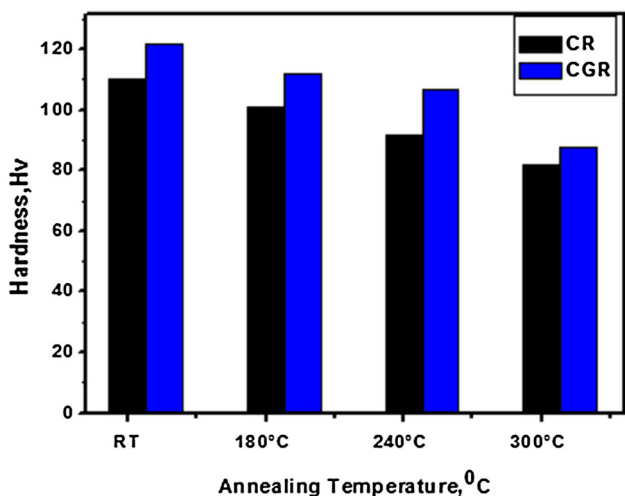


**Fig. 10** Effect of annealing temperature on hardness of 90% CR, CGR reductions

ST samples from 249 to 29 kJ/m<sup>2</sup>. In case of CGR samples, it is decreased to 112 kJ/m<sup>2</sup> in 50% CGR samples, but gradually increased to 142 kJ/m<sup>2</sup> in 75% CGR samples. It is

due to strain hardening in the material during CGR, which leads to decrease in ductility as well as fracture toughness of the alloy. It was reported for ECAP processed Al–Mg and Al–Cu that its static toughness decreases significantly due to decrease in its elongation than its casting state, although its strength is obviously increased [13, 47]. It is observed that the  $J_{integral}$  of the ST sample shows a larger value, 249 kJ/m<sup>2</sup>, when compared to its bulk counterpart, owing to the formation of dislocation-free equiaxed coarse grains. It imparts improved ductility and fracture toughness to the ST alloy.

SEM fractographs of three-point bending test samples shown in Fig. 7 reveal that the ST samples with larger dimples are due to ductile fracture, due to which  $J_{integral}$  value is more, revealing the delay in crack propagation in coarser grains [44]. The 50 and 75% CR samples possess fine dimples, indicating the mixed mode of fracture, which indicate the gradual decrease of  $J_{integral}$  value, whereas in case of 50% CGR and 75% CGR samples, dimple size are comparatively larger than CR samples, which is responsible for better fracture toughness.

**Fig. 11** SEM fractographs of AA 5052 at ×5000 magnification after Tensile test (a) CR + annealed alloy at 180 °C (b) CR + annealed at 240 °C (c) CR + annealed at 300 °C (a') CGR + annealed at 180 °C (b') CGR + annealed at 240 °C (c') CGR + annealed at 300 °C

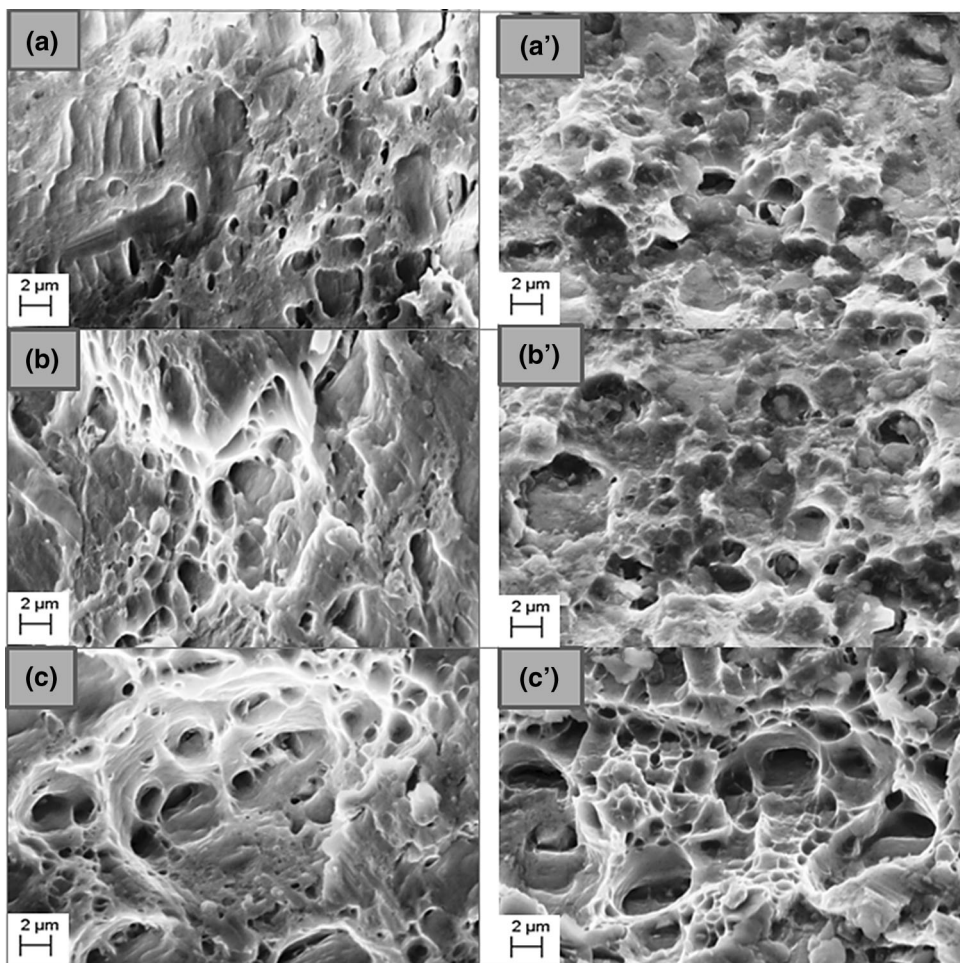


**Fig. 12** SEM fractographs of AA 5052 after three-point bending test (a) CR + annealed at 180 °C (b) CR + annealed at 240 °C (c) CR + annealed at 300 °C (a') CGR + annealed at 180 °C (b') CGR + annealed at 240 °C (c') CGR + annealed at 300 °C

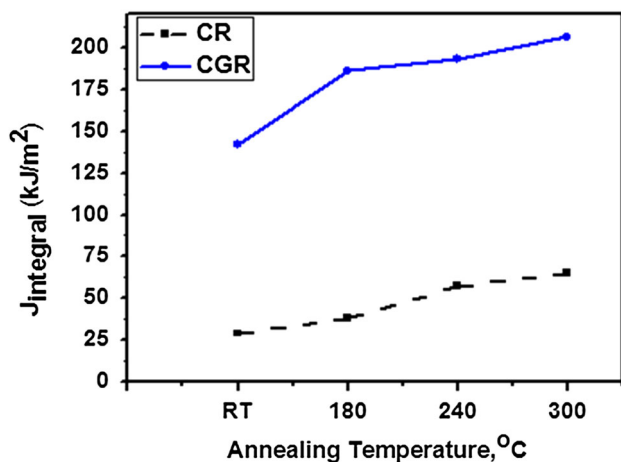
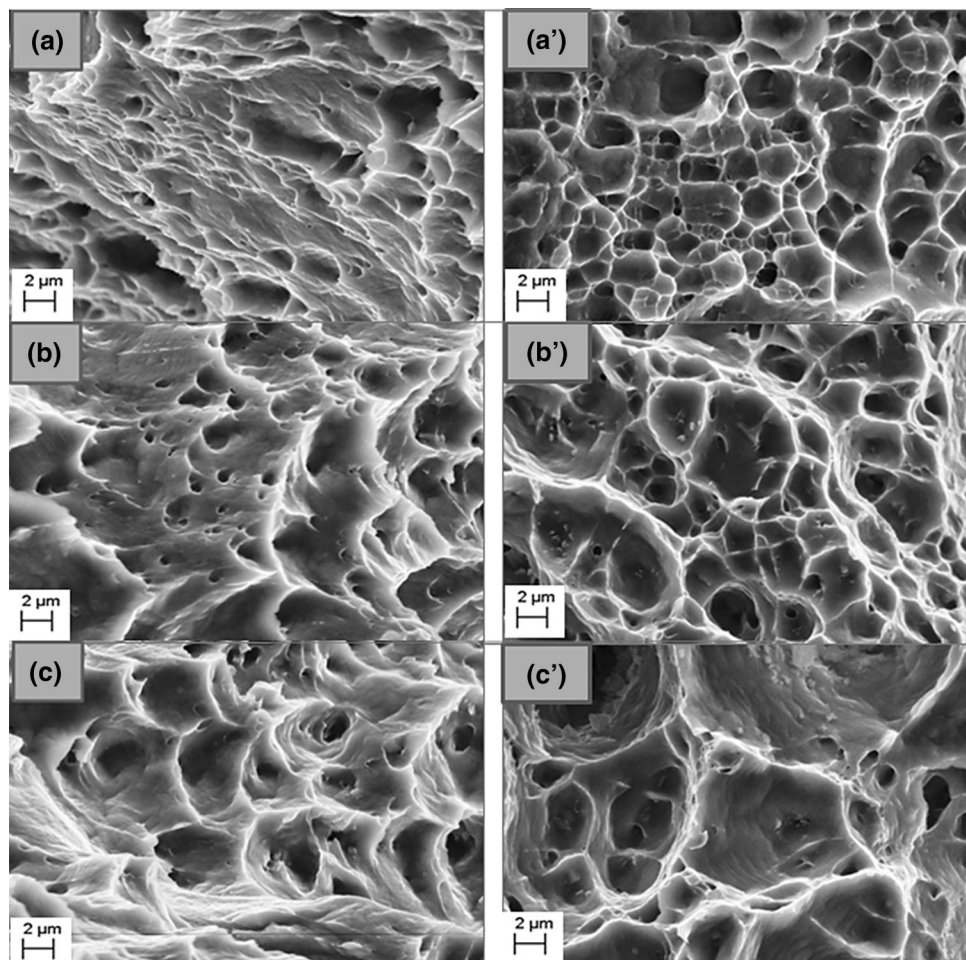


**Fig. 13** Variation in  $J_{\text{integral}}$  with respect to annealing temperature in 75% rolled samples

### XRD Analysis

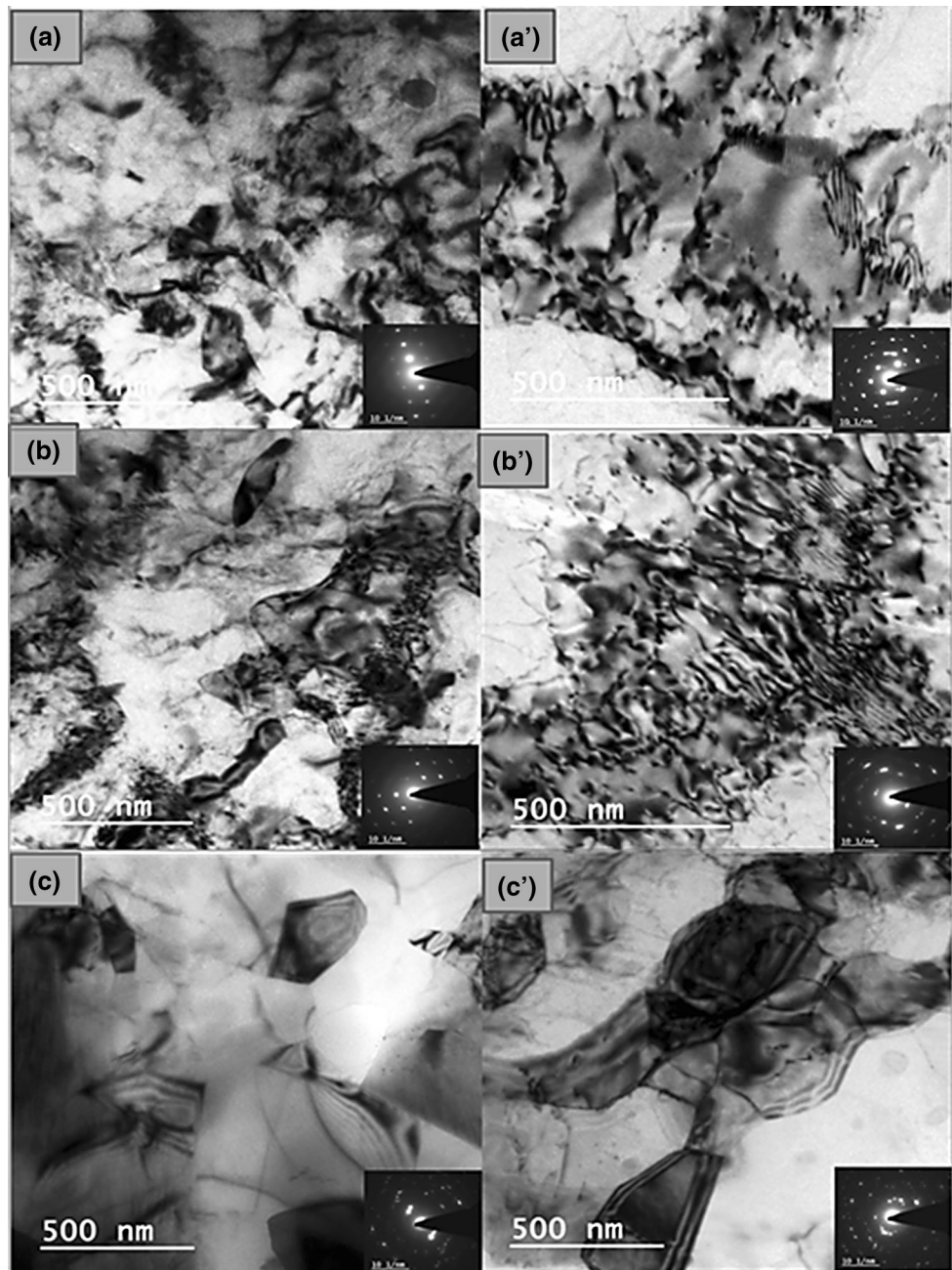
XRD peaks (Fig. 8) show that there is a drastic decrease in the peaks of (1 1 1) and (2 0 0) orientation. Also,

there is a preferred orientation for the rolled samples along (2 2 0) plane. The peak corresponding to 90% CGR samples is comparatively larger than 90% CR samples, which is attributed to the accumulation of strain in the rolling direction [48]. The peak shift and peak broadening for 90% CGR samples reveal the grains are finer than 90% CR samples. The smaller peaks correspond to impurity phase particles ( $\text{Mg}_2\text{Si}$ ,  $\text{MgO}$ ), which promote dislocation accumulation through effective pinning of dislocation [49].

### Post-Annealing Observations

The post-deformation annealed samples show the formation of recovered grains. With increasing annealing temperature from 180 to 300 °C, the dislocation density in both CR and CGR samples are decreasing due to the formation of sub-grains occurring through recovery process [2]. In the post-deformed samples, the percentage of elongation to failure has increased from 6 to 12%, in 90% CR samples and 3 to 12% in CGR samples (Fig. 9c and Table 3). The

**Fig. 14** TEM images with SAED pattern of AA 5052: 90% cryorolled followed by annealing at 240 °C (a) 75%CR, (b) 90%CR (c) CR + annealed at 240 °C (a') 75%CGR (b') 90%CGR (c') CGR + annealed at 240 °C



tensile strength (Fig. 9a) and hardness values (Fig. 10) have decreased from 291 to 160 MPa & 110 to 82 HV in 90% CR samples and 315–172 MPa & 122 to 88 HV in 90% CGR samples, respectively. It is attributed to the formation of sub-grains and rearrangement of dislocations including some loss of dislocations as the recovery proceeds. SEM fractography of both tensile test (Fig. 11) and three-point bending test (Fig. 12) of the post-annealed samples show larger dimple. The CGR samples show slightly larger dimples than CR samples, which is responsible for the improvement of ductility. Due to increase in ductility, the fracture toughness ( $J_{\text{integral}}$ ) value for the

annealed samples has increased from 29.1 to 65.1 kJ/m<sup>2</sup> in 75%CR samples and 142 kJ/m<sup>2</sup> to 206 kJ/m<sup>2</sup> in 75% CGR samples (Fig. 13), which are annealed between the temperature 180 and 300 °C.

#### TEM Analysis

The TEM images (Fig. 14) of 90% CR samples show parallel bands of severely elongated substructure containing high density of dislocations, whereas the 90% CGR samples possess a much more dislocation density. The heavily strained sub-grains are observed in both

conditions. In the heavily deformed grains of CGR samples, dislocation cells, dense dislocation walls, and dislocation-tangling zone, were also observed. However, in CR samples, relatively low dislocation density with well-defined sub-grains is observed. The similar observations were made by Panigrahi et al. for CR samples at true strain of 3.8 and Krishna et al. [37, 48]. The elongated spots in the SAED patterns reveal the better refinement in 90% CGR samples than 90% CR samples. The post-annealed (240 °C) samples reveal the formation of bimodal microstructure consisting of elongated sub-grains and small equiaxed grains in both CR and CGR samples. These freshly recrystallized grains are free from dislocation and are of various sizes due to abnormal grain growth occurring at 240 °C. In case of CGR samples, this combination of coarse grain (size around 0.5 µm) and ultrafine grain (size around 200 nm) are better in proportion than CR samples so as to withstand fracture growth.

## Conclusions

AA 5052 subjected to cryorolling and cryo groove rolling with different thickness reduction and post-annealing treatment has been investigated for understanding its tensile and fracture behavior. The detailed microstructural characterizations of the deformed and annealed samples were made. The following conclusions are made based on the present study.

- The significant increase in the ultimate tensile strength up to 291 MPa has been observed in 90% CR samples when compared to ST (170 MPa), whereas in 90% CGR samples, it has improved to 313 MPa. It is due to the combined effect of compression and shear stress, which leads to better dislocation strengthening, sub-grain formation, and grain size effect in CGR samples as compared to CR samples. The ductility of the deformed alloy has improved from 6 to 12% in CR samples and 3 to 12% in CGR samples after post-annealing treatment due to partial recovery of the deformed alloy.
- Similarly, the hardness value has increased from 55 to 110 and 122 Hv, respectively, in 90% CR and 90% CGR samples. This notable improvement in strength and hardness is attributed to accumulation of high dislocation density during CGR process.
- The optical images corresponding to the 90% CGR samples possess highly dense dislocation cell network than 90% CR samples, which are responsible for the refinement of grain and hence its improved mechanical properties.
- The fracture toughness of 75% CGR samples is higher (142 kJ/m<sup>2</sup>) than the 75% CR samples (29 kJ/m<sup>2</sup>) as evident from the SEM fractography of the three-point bending test samples. The CGR samples show a slightly larger dimples than CR samples and therefore exhibit higher fracture toughness value compared to CR samples.

## References

1. D. Singh, P.N. Rao, R. Jayaganthan, Effect of deformation temperature on mechanical properties of ultrafine grained Al–Mg alloys processed by rolling. *Mater. Des.* **50**, 646–655 (2013)
2. U.G. Kang, J.C. Lee, S.W. Jeong, W.J. Nam, The improvement of strength and ductility in ultra-fine grained 5052 Al alloy by cryogenic-and warm-rolling. *J. Mater. Sci.* **45**(17), 4739–4744 (2010)
3. H.R. Song, Y.S. Kim, W.J. Nam, Mechanical properties of ultra-fine grained 5052 Al alloy produced by accumulative roll-bonding and cryogenic rolling. *Met. Mater. Int.* **12**(1), 7–12 (2006)
4. S.H. Lee, Y. Saito, T. Sakai, H. Utsunomiya, Microstructures and mechanical properties of 6061 aluminum alloy processed by accumulative roll-bonding. *Mater. Sci. Eng. A* **325**(1), 228–235 (2002)
5. N. Tsuji, Y. Saito, S.H. Lee, ARB (accumulative roll-bonding) and other new techniques to produce bulk ultrafine grained materials. *Adv. Eng. Mater.* **5**(5), 338–344 (2003)
6. Y. Saito, H. Utsunomiya, N. Tsuji, T. Sakai, Novel ultra-high straining process for bulk materials—development of the accumulative roll-bonding (ARB) process. *Acta Materialia* **47**(2), 579–583 (1999)
7. M. Ruppert, C. Schunk, D. Hausmann, H.W. Höppel, Global and local strain rate sensitivity of bimodal Al-laminates produced by accumulative roll bonding. *Acta Mater.* **103**, 643–650 (2016)
8. S.O. Gashti, A. Fattah-alhosseini, Y. Mazaheri, Effects of grain size and dislocation density on strain hardening behavior of ultrafine grained AA1050 processed by accumulative roll bonding. *J. Alloy. Compd.* **658**, 854–861 (2016)
9. M. Eizadjou, A.K. Talachi, H.D. Manesh, Investigation of structure and mechanical properties of multi-layered Al/Cu composite produced by accumulative roll bonding (ARB) process. *Compos. Sci. Technol.* **68**(9), 2003–2009 (2008)
10. Y.C. Chen, Y.Y. Huang, C.P. Chang, P.W. Kao, The effect of extrusion temperature on the development of deformation microstructures in 5052 aluminium alloy processed by equal channel angular extrusion. *Acta Mater.* **51**(7), 2005–2015 (2003)
11. A. Chatterjee, G. Sharma, A. Sarkar, J.B. Singh, A study on cryogenic temperature ECAP on the microstructure and mechanical properties of Al–Mg alloy. *Mater. Sci. Eng. A* **556**, 653–657 (2012)
12. A. Nashith, P. Sanjid, M. Shamsudheen, Effect of equal channel angular pressing (ECAP) on hardness and microstructure of pure aluminum. *Int. J. Mater. Eng.* **4**(3), 119–122 (2014)
13. D.R. Fang, Q.Q. Duan, N.Q. Zhao, J.J. Li, S.D. Wu, Tensile properties and fracture mechanism of Al–Mg alloy subjected to equal channel angular pressing. *Mater. Sci. Eng. A* **459**(1), 137–144 (2007)
14. A. Mogucheva, D. Yuzbekova, Superplasticity in a 5024 aluminium alloy subjected to ECAP and subsequent cold rolling. *Mater. Sci. Forum. Trans. Tech. Publ.* **838**, 428–433 (2016)
15. Y. Duan, L. Tang, G. Xu, Y. Deng, Z. Yin, Microstructure and mechanical properties of 7005 aluminum alloy processed by room temperature ECAP and subsequent annealing. *J. Alloy. Compd.* **664**, 518–529 (2016)

16. M. Murashkin, A. Medvedev, V. Kazykhanov, A. Krokhin, Enhanced mechanical properties and electrical conductivity in ultrafine-grained Al 6101 alloy processed via ECAP-conform. *Metals* **5**(4), 2148–2164 (2015)
17. P.N. Rao, D. Singh, R. Jayaganthan, Mechanical properties and microstructural evolution of Al 6061 alloy processed by multi-directional forging at liquid nitrogen temperature. *Mater. Des.* **56**, 97–104 (2014)
18. Z. Xiaoming, Z. Tingjie, T. Feng, L. Zhongkui, Effects of multi-direction forging on improving properties of 7075 aluminum alloy. *Rare Metal Mater. Eng.* **32**(5), 372–374 (2003)
19. M. Noda, M. Hirohashi, K. Funami, Low temperature superplasticity and its deformation mechanism in grain refinement of Al-Mg alloy by multi-axial alternative forging. *Mater. Trans.* **44**(11), 2288–2297 (2003)
20. B. Cherukuri, R. Srinivasan, Properties of AA6061 processed by multi-axial compressions/forging (MAC/F). *Mater. Manuf. Process.* **21**(5), 519–525 (2006)
21. M. Montazeri-Pour, M.H. Parsa, H.R. Jafarian, Microstructural and mechanical properties of AA1100 aluminum processed by multi-axial incremental forging and shearing. *Mater. Sci. Eng. A* **639**, 705–716 (2015)
22. Y.T. Zhu, T.C. Lowe, H. Jiang, J. Huang, Method for producing ultrafine-grained materials using repetitive corrugation and straightening. U.S. Patent No. 6, 197,129 (2001)
23. V. Rajinikanth, G. Arora, N. Narasaiah, K. Venkateswarlu, Effect of repetitive corrugation and straightening on Al and Al–0.25 Sc alloy. *Mater. Lett.* **62**(2), 301–304 (2008)
24. S.C. Pandey, M.A. Joseph, M.S. Pradeep, A theoretical and experimental evaluation of repetitive corrugation and straightening: application to Al–Cu and Al–Cu–Sc alloys. *Mater. Sci. Eng. A* **534**, 282–287 (2012)
25. J.K. McBride, R.E. Sanders, H.G. Reavis, The development of 5XXX aluminum alloys for RCS applications. *JOM* **48**(6), 18–21 (1996)
26. Y.T. Zhu, H. Jiang, J. Huang, T.C. Lowe, A new route to bulk nanostructured metals. *Metall. Mater. Trans. A* **32**(6), 1559–1562 (2001)
27. J. Huang, Y.T. Zhu, D.J. Alexander, X. Liao, Development of repetitive corrugation and straightening. *Mater. Sci. Eng. A* **371**(1), 35–39 (2004)
28. Z. Horita, T.G. Langdon, Microstructures and microhardness of an aluminum alloy and pure copper after processing by high-pressure torsion. *Mater. Sci. Eng. A* **410**, 422–425 (2005)
29. G. Sakai, Z. Horita, T.G. Langdon, Grain refinement and superplasticity in an aluminum alloy processed by high-pressure torsion. *Mater. Sci. Eng. A* **393**(1), 344–351 (2005)
30. C. Xu, Z. Horita, T.G. Langdon, The evolution of homogeneity in an aluminum alloy processed using high-pressure torsion. *Acta Mater.* **56**(18), 5168–5176 (2008)
31. A. Loucif, R.B. Figueiredo, T. Baudin, F. Brisset, Microstructural evolution in an Al-6061 alloy processed by high-pressure torsion. *Mater. Sci. Eng. A* **527**(18), 4864–4869 (2010)
32. A. Loucif, Y. Huang, A.L. Helbert, T. Baudin, Microtextural changes and superplasticity in an Al-7075 alloy processed by high-pressure torsion. *Mater. Sci. Forum Trans. Tech. Publ.* **838**, 445–450 (2016)
33. H. Iwaoka, Z. Horita, High-pressure torsion of thick Cu and Al–Mg–Sc ring samples. *J. Mater. Sci.* **50**(14), 4888–4897 (2015)
34. A. Alhamidi, Z. Horita, Grain refinement and high strain rate superplasticity in aluminium 2024 alloy processed by high-pressure torsion. *Mater. Sci. Eng. A* **622**, 139–145 (2015)
35. Y.B. Lee, D.H. Shin, W.J. Nam, Effect of annealing temperature on tensile behavior of 5052 Al alloy deformed at cryogenic temperature. *J. Mater. Sci.* **40**(5), 1313–1315 (2005)
36. D. Singh, P.N. Rao, R. Jayaganthan, Microstructures and impact toughness behavior of Al 5083 alloy processed by cryorolling and afterwards annealing. *Int. J. Miner Metall. Mater.* **20**(8), 759–769 (2013)
37. S.K. Panigrahi, R. Jayaganthan, Development of ultrafine-grained Al 6063 alloy by cryorolling with the optimized initial heat treatment conditions. *Mater. Des.* **32**(4), 2172–2180 (2011)
38. N. Kumar, P.N. Rao, R. Jayaganthan, H.G. Brokmeier, Effect of cryorolling and annealing on recovery, recrystallisation, grain growth and their influence on mechanical and corrosion behaviour of 6082 Al alloy. *Mater. Chem. Phys.* **165**, 177–187 (2015)
39. A. Dhal, S.K. Panigrahi, M.S. Shunmugam, Influence of annealing on strain hardening behaviour and fracture properties of a cryorolled Al 2014 alloy. *Mater. Sci. Eng. A* **645**, 383–392 (2015)
40. J. Marnette, M. Weiss, P.D. Hodgson, Roll-formability of cryorolled ultrafine aluminium sheet. *Mater. Des.* **63**, 471–478 (2014)
41. W. Bo, X. Chen, F. Pan, J. Mao, F. Yong, Effects of cold rolling and heat treatment on microstructure and mechanical properties of AA 5052 aluminum alloy. *Trans. Nonferrous Metals Soc. China* **25**(8), 2481–2489 (2015)
42. J.W. Lee, J.J. Park, Numerical and experimental investigations of constrained groove pressing and rolling for grain refinement. *J. Mater. Process. Technol.* **130**, 208–213 (2002)
43. A. Krishnaiah, U. Chakkingal, P. Venugopal, Production of ultrafine grain sizes in aluminium sheets by severe plastic deformation using the technique of groove pressing. *Scripta Mater.* **52**(12), 1229–1233 (2005)
44. Z. Lee, V. Radmilovic, B. Ahn, E.J. Lavermia, Tensile deformation and fracture mechanism of bulk bimodal ultrafine-grained Al-Mg alloy. *Metall. Mater. Trans. A* **41**(4), 795–801 (2010)
45. ASTM E1820-01, Standard Test Method for Measurement of Fracture Toughness. ASTM International, West Conshohocken, 1036–1081 (2005)
46. T. Inoue, Y. Kimura, S. Ochiai, Static fracture toughness of fail-safe steel. *Scr. Mater.* **65.6**, 552–555 (2011)
47. D.R. Fang et al., Effects of equal channel angular pressing on the strength and toughness of Al–Cu alloys. *J. Mater. Sci.* **46**(14), 5002–5008 (2011)
48. N.N. Krishna, M. Ashfaq, P. Susila, K. Sivaprasad, Mechanical anisotropy and microstructural changes during cryorolling of Al–Mg–Si alloy. *Mater. Charact.* **107**, 302–308 (2015)
49. W.X. Wang, P. Liu, L.T. Gan, Research on friction and wear properties of annealed 5052 Al-Mg alloy. *Adv. Mater. Res.* **160**, 157–162 (2011)